

Rangan, Rajiv, miRNA Profiling of Human Optic Nerve Head Astrocytes Exposed to Cyclic Stretch. Master of Science (Medical Sciences Research Track), April 2021, 26 pp.; 2 tables, 6 figures, bibliography.

### **Summary**

Glaucoma is a leading cause of irreversible blindness. Vision loss results from the degeneration and death of retinal ganglion cells (RGCs) and their axons. The primary risk factor for glaucoma is increased intraocular pressure (IOP) (2). Elevated IOP results in aberrations in the biomechanical properties of ocular tissues – including the transmission of biomechanical stretch through the reticulated, fibroelastic region of the optic nerve head (ONH) known as the lamina cribrosa (LC) (6). Cells of the LC are sensitive to biomechanical stretch and respond to increased stretch and pressure to promote the excessive synthesis of extracellular matrix (ECM) proteins and ECM remodeling (15,17). These responses promote a fibrotic environment within the LC that can cause mechanical damage to the axons of RGCs. ONH astrocytes represent one of the major cell types of the LC and are believed to contribute significantly to pathological ECM remodeling at the LC during glaucoma (11). ONH astrocytes also demonstrate a dysregulated pattern of protein expression when exposed to stretch (17). The mechanism that underlies this stretch-induced, aberrant dysregulation is unknown. MicroRNA (miRNA) dysregulation may represent one of the mechanisms contributing to the differential protein expression patterns seen in ONH astrocytes exposed to stretch. In this study we examine the miRNA profiles of ONH astrocytes exposed to cyclic stretch.

## **Hypothesis**

Glaucoma pathogenesis is associated with elevated IOP and remodeling of the ECM in the LC of the ONH. ONH astrocytes are one of the major cell types responsible for ECM remodeling in the LC (11). Our laboratory has provided evidence for the role of miRNAs in glaucoma. We have demonstrated that the profibrotic cytokine transforming growth factor-beta 2 (TGF $\beta$ 2) increases profibrotic miRNAs and decreases anti-fibrotic miRNAs in ONH cells. This suggests that miRNAs are involved in creating a profibrotic environment in the LC. Given the demonstrable sensitivity of ONH astrocytes to stretch and the profibrotic environment of the LC that develops under conditions of elevated IOP, we hypothesize that biomechanical stretch dysregulates miRNAs resulting in an increase of profibrotic miRNAs and a decrease of anti-fibrotic miRNAs in ONH astrocytes (Figure 1).

## **Significance**

Currently, the available therapeutics for glaucoma are designed to lower IOP. This effectively slows glaucoma progression in many individuals but cannot stop or reverse vision loss (4). Understanding the role of ONH astrocyte activation in response to biomechanical signals will help develop a complete picture of glaucoma pathogenesis. Additionally, the characterization of dysregulated miRNA expression may help identify new therapies using miRNA mimics and antagomirs. As pointed out by Hanna et al., nonprotein coding genes operate in diverse manners and affect a multitude of targets. This makes drugs modeled after non-coding RNAs particularly well-suited for diseases with complex etiologies and warrants their further study in the context of disease processes (35).

MIRNA PROFILING OF HUMAN OPTIC NERVE HEAD

ASTROCYTES EXPOSED TO CYCLIC STRETCH

Rajiv Rangan, B.S.

APPROVED:

---

Tara Tovar-Vidales, Ph.D., Major Professor

---

Abe Clark, Ph.D., Committee Member

---

Yang Liu, Ph.D., Committee Member

---

Caroline Rickards, Ph.D., Program Director

---

Lisa Hodge, Ph.D., Assistant Dean for Specialized MS Programs

---

J. Michael Mathis, Ph.D., Ed.D., Dean

Graduate School of Biomedical Sciences

# miRNA Profiling of Human Optic Nerve Head Astrocytes Exposed to Cyclic Stretch

**Research Practicum Final Report**

Rajiv Rangan

Masters of Science in Medical Sciences Research Track

Graduate School of Biomedical Sciences

Mentor: Tara Tovar-Vidales, PhD

## Acknowledgments

I would first like to thank my mentor Dr. Tara Tovar-Vidales for her constant patience and kindness. She has provided me with an invaluable amount of training and guidance over the year. I would like to thank my committee members, Dr. Yang Liu and Dr. Abe Clark, for always being willing to take the time to provide me with their help, insights and life advice. I also appreciate all of the help and support I received from Dr. Navita Lopez, whose work was foundational to much of this project. Finally I would like to thank all of the warm and welcoming faculty I have had the pleasure of knowing at UNTHSC & The North Texas Eye Research Institute; especially Dr. Denise Inman, Dr. Dorota Stankowska and Dr. Raghu Krishnamoorthy. This year has been incredibly formative, and I will forever be grateful for the experience I have had at NTERI.

## TABLE OF CONTENTS

<b>Acknowledgments .....</b>	<b>1</b>
<b>Table of Contents .....</b>	<b>2</b>
<b>List of Tables .....</b>	<b>3</b>
<b>List of Figures.....</b>	<b>4</b>
<b>Background .....</b>	<b>5</b>
<b>Methods.....</b>	<b>9</b>
<b>Results .....</b>	<b>14</b>
<b>Discussion.....</b>	<b>20</b>
<b>Limitations.....</b>	<b>25</b>
<b>References .....</b>	<b>27</b>

## List of Tables

<b>Table 1</b> .....	<b>12</b>
Primary Antibody Information	
<b>Table 2</b> .....	<b>16</b>
Dysregulated miRNAs and Predicted Targets	

## List of Figures

<b>Figure 1</b> .....	<b>8</b>
Hypothesis	
<b>Figure 2</b> .....	<b>11</b>
Layout of Pathway-Focused miScript miRNA PCR Array for Human Fibrosis	
<b>Figure 3</b> .....	<b>16</b>
Differential mature miRNA expression patterns detected in three independent primary human ONHA cell cultures exposed to 0-12% cyclic stretch for 24 hours	
<b>Figure 4</b> .....	<b>18</b>
Western Blot Results	
<b>Figure 5</b> .....	<b>19</b>
Western Blot Optical Density Quantitation	
<b>Figure 6</b> .....	<b>23</b>
Predicted miRNA Interactions	

## **Background**

Glaucoma categorizes a heterogeneous group of ocular diseases and results in the progressive loss of RGCs and their axons (1). Glaucoma is relatively common in older populations - by some estimates, 1 in 40 individuals above the age of 40 will experience vision loss due to glaucoma (2). Glaucoma is typically painless and otherwise asymptomatic. Detection of glaucoma often only occurs later in the disease process when peripheral vision loss becomes apparent. Vision lost due to glaucoma is currently irreversible (2). The primary risk factor for glaucomatous optic neuropathies is elevated IOP (3). The only available glaucoma treatments are all targeted towards reducing IOP – these therapeutics cannot reverse or stop glaucoma, but are effective in slowing its progression (4).

In glaucoma, damage to the RGC axons first occurs at the LC of the ONH, where bundles of RGC axons pass through pores in the region's layers of fibroelastic plates (5). The LC is a distinct region of the ONH composed of a network of connective and vascular tissues, and distinct cell populations (6). The two major cell types of the LC, which predominate cultures of explanted LC tissue, are the GFAP negative LC cells and the GFAP positive ONH astrocytes (ONHA) (7). Cells of the LC may contribute to RGC axonal damage and apoptotic cell death, in part, via the pathological remodeling of the ECM. Excessive production of ECM proteins creates a profibrotic environment that promotes the mechanical damage of RGCs, leading to axonal degeneration accompanied by apoptotic RGC death (2). For example, TGF $\beta$ 1 is a profibrotic mediator with a physiologic role in ocular wound healing that has been found to become dysregulated during fibrosis and is strongly implicated in the pathogenesis of glaucoma (8,9). When LC cells are exposed to TGF $\beta$ 1, they demonstrate increased expression of ECM proteins

such as collagen IV, collagen I and elastin, as well as an increased expression of matrix metalloproteinase inhibitors (10).

ONHA also contribute to pathological ECM remodeling in the LC region. Astrocytes are the main glial cell population of the ONH and are normally “quiescent,” acting to support and nourish associated axons of the RGCs (11). When a neural injury occurs, through trauma or disease, astrocytes shift into a “reactive” state – a process called “astrogliosis” that normally serves to prevent damage to intact neurons (12). Reactive ONHA seem to participate in ONH remodeling and promote RGC axonal degeneration (11). One factor that might promote the transition of ONHA from quiescent to reactive is biomechanical stretch. During glaucoma progression, IOP increases are associated with cupping of the optic disc and posterior bowing of the optic nerve. These morphological changes result from and contribute to mechanical distortions in the ONH tissues, including the transmission of stretch through the LC (13). Both major cell populations of the LC – LC cells and ONHA – are sensitive to biomechanical signals such as pressure and stretch, and their responses frequently include the upregulation of ECM-associated proteins (14, 15, 16). In this proposed study, we will focus our examination on the response of ONHA to biomechanical stretch with a focus on how these responses relate to ECM remodeling. A proteomics study conducted by Rogers et al. has previously demonstrated that multiple molecular pathways become dysregulated in ONHA exposed to biomechanical stretch (17), but the mechanisms by which stretch induces changes in protein expression are not fully understood.

One mechanism by which stretch induces changes in protein expression may be through miRNAs. miRNAs are an important group of regulatory molecules that act primarily through post-transcriptional mRNA translation inhibition (18). miRNAs are initially transcribed from

specific genes as long, primary miRNA molecules (pri-miRNA). pri-miRNA molecules are cleaved by the ribonuclease Drosha, which results in the formation of hairpin-structured pre-miRNA molecules (18). The ribonuclease Dicer cleaves and further processes pre-miRNA molecules into double-stranded RNA molecules that will ultimately be processed into mature single-stranded miRNA (19). Mature miRNA molecules integrate with the RNA-induced silencing complex (RISC) and can imperfectly base pair with the 3'-untranslated or coding regions of multiple mRNA transcripts, causing the inhibition of protein translation (20). As a result, changes in miRNA expression profiles can shape the proteomic landscape of cells. The dysregulated expression of miRNAs has been demonstrated to play a role in many disease processes, including fibrosis and neurodegeneration (21, 22). Members of the miR-29 family are expressed broadly by neurons and astrocytes of the brain and target the beta-secretase 1 precursor protein. Reduced expression of miR-29 is believed to contribute to the development of beta-amyloid plaques, fibrosis and neuronal damage during Alzheimer's progression (23). Similarly, in molecular models of glaucoma progression, the profibrotic mediator TGF $\beta$ 2 has been demonstrated to modulate the expression of miR-29a, miR-29b and miR-29c in trabecular meshwork cells; this may have important implications for how aqueous humor dynamics are pathologically altered (24).

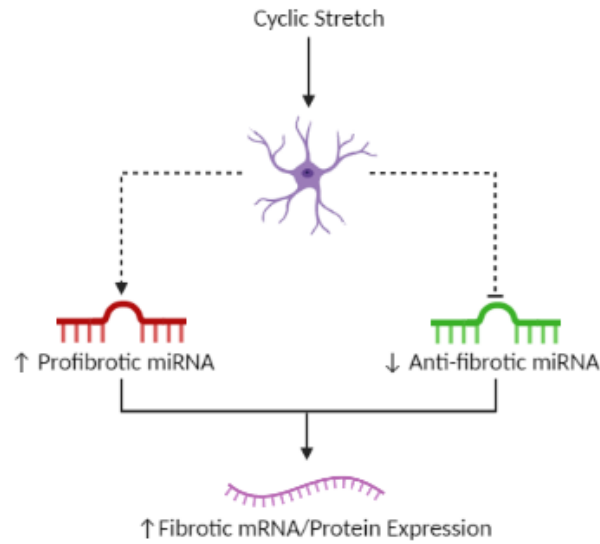


**Figure 1. Hypothesis**

Hypothesized mechanism for the role of miRNAs in the regulation of fibrotic protein expression. Created with BioRender.com

In this study, we analyzed the effects of biomechanical stretch, applied cyclically at 0-12% for 24 hours, on the miRNA expression profile of ONHA. We focused on the pro- and anti-fibrotic miRNAs and employed bioinformatics tools such as TargetScan (25) to assess whether miRNAs with significantly altered expression can be putatively associated with proteins involved in ECM remodeling. We also collected conditioned medium samples from the ONHA to analyze the effects of stretch on fibrotic proteins. Our results may help further elucidate the molecular pathways by which astrocytes become activated, the pathways by which stretch influences ECM remodeling and ultimately how IOP modulates ONH cellular responses during glaucoma progression. Further, the characterization of dysregulated miRNA profiles may help identify new drug targets and models for novel therapeutic compounds.

## **Methods**

### *Cells Culture*

Primary human ONHA were previously isolated and characterized using techniques described by Lopez et al. (27). All cells were grown in astrocyte medium (ScienCell Research Laboratories, Carlsbad, CA) supplemented with 5% FBS (Peak Serum, Wellington, CO), astrocyte growth supplement and penicillin/streptomycin solution (ScienCell). The medium was changed biweekly and cells were kept in 37°C and 5% CO<sub>2</sub> incubators.

### *Stretch Experiments*

In preparation for the stretch experiments, ~8.0 x 10<sup>4</sup> ONHA were plated on precoated collagen IV BioFlex® 6-well flex culture plates. Cells were allowed to grow on the flex plates until confluent. Then, cells were serum-deprived for 24 hours (followed by fresh serum-free medium) prior to the start of stretch experiments.

Half the cohort of ONHA were subjected to cyclic stretch, while the other half were not subjected to stretch (0% stretch controls). Cells in the treatment group were exposed to cyclic stretch for 24-hours on a baseplate attached to a FlexCell® FX-6000T™ programmable system. This programmable system applies cyclic stretch to culture plates by a vacuum pump system. The device was programmed for cells to be cyclically exposed to 0-12% stretch at a frequency of 1Hz.

### *RNA Isolation*

Total RNA was extracted from ONHA for use in downstream analysis of miRNA expression profiles by real-time PCR. Conditioned medium was removed and stored at -20°C for later analysis and cells were washed with warm phosphate-buffered saline. ONHA were then dissociated from the collagen IV coated wells with TrypLE Express (ThermoFisher, Waltham, MA). Cells were collected and pelleted by centrifugation at 1000 RCF for 5 minutes, before being resuspended in 700µl QIAzol Lysis Reagent (Qiagen, Hilden, Germany). RNA isolation was conducted using the spin column extraction protocol established for the commercial miRNeasy Mini Kit (Qiagen). The Nanodrop 2000 (Thermofisher) was used to confirm RNA purity via 260/280 ratios.

### *cDNA Synthesis and Real-Time PCR*

cDNA was synthesized from total RNA samples using the miScript II Reverse Transcriptase Kit using the HiSpec Buffer protocol for mature miRNA expression profiling (Qiagen). Synthesized cDNA served as a template for conducting real-time PCR arrays with miScript SYBR green reaction mix and the 96-well miScript miRNA PCR array for human fibrosis – depicted in Figure 2 (MIHS-117Z; Qiagen). Raw data collection and baseline threshold normalization were conducted using the BioRad ThermoCycler's CFX Maestro software (BioRad, Hercules, CA).



**Figure 2. Layout of Pathway-Focused miScript miRNA PCR Array for Human Fibrosis**

The miScript miRNA PCR array for human fibrosis is designed to profile the expression of miRNAs that have mRNA targets in fibrotic pathways. The miRNAs profiled by this array may be involved in the following pathway categories: pro-fibrotic, anti-fibrotic, extracellular matrix & cell adhesion, inflammation, angiogenesis, signal transduction & transcriptional regulation. The wells in rows A-G contain primers for the following mature miRNAs: hsa-let-7d-5p, hsa-miR-1-3p, hsa-miR-101-3p, hsa-miR-107, hsa-miR-10a-5p, hsa-miR-10b-5p, hsa-miR-122-5p, hsa-miR-125b-5p, hsa-miR-126-3p, hsa-miR-129-5p, hsa-miR-132-3p, hsa-miR-133a-3p, hsa-miR-141-3p, hsa-miR-142-3p, hsa-miR-143-3p, hsa-miR-145-5p, hsa-miR-146a-5p, hsa-miR-146b-5p, hsa-miR-148a-3p, hsa-miR-150-5p, hsa-miR-155-5p, hsa-miR-15b-5p, hsa-miR-16-5p, hsa-miR-17-5p, hsa-miR-18a-5p, hsa-miR-192-5p, hsa-miR-194-5p, hsa-miR-195-5p, hsa-miR-196a-5p, hsa-miR-199a-5p, hsa-miR-199b-5p, hsa-miR-19a-3p, hsa-miR-19b-3p, hsa-miR-200a-3p, hsa-miR-200b-3p, hsa-miR-203a-3p, hsa-miR-204-5p, hsa-miR-208a-3p, hsa-miR-20a-5p, hsa-miR-21-5p, hsa-miR-211-5p, hsa-miR-215-5p, hsa-miR-216a-5p, hsa-miR-217, hsa-miR-223-3p, hsa-miR-23a-3p, hsa-miR-25-3p, hsa-miR-26a-5p, hsa-miR-26b-5p, hsa-miR-27a-3p, hsa-miR-27b-3p, hsa-miR-29a-3p, hsa-miR-29b-3p, hsa-miR-29c-3p, hsa-miR-302b-3p, hsa-miR-30a-5p, hsa-miR-31-5p, hsa-miR-32-5p, hsa-miR-324-5p, hsa-miR-324-3p, hsa-miR-325, hsa-miR-328-3p, hsa-miR-335-5p, hsa-miR-338-5p, hsa-miR-34a-5p, hsa-miR-372-3p, hsa-miR-375, hsa-miR-377-3p, hsa-miR-378a-3p, hsa-miR-382-5p, hsa-miR-449a, hsa-miR-449b-5p, hsa-miR-451a, hsa-miR-491-5p, hsa-miR-5011-5p, hsa-miR-503-5p, hsa-miR-5692a, hsa-miR-590-5p, hsa-miR-661, hsa-miR-663a, hsa-miR-7-5p, hsa-miR-744-5p, hsa-miR-874-3p, hsa-miR-92a-3p. Wells H1-2 are *C. elegans* miR-39 miScript primer assays, wells H3-8 are snoRNA/snRNA miScript PCR controls, wells H9-10 are reverse transcription controls and wells H11-12 are positive PCR controls (Qiagen).

### *miRNA Expression Profile Analysis*

miRNA PCR array data was processed using the GeneGlobe miRNA PCR array analysis tool (<https://geneglobe.qiagen.com/us/analyze/>). Through this tool, data across samples were normalized by the arithmetic  $C_T$  mean of the SNORD96A housekeeping gene. The GeneGlobe analysis tool was used to determine the significance of differences in  $\Delta C_T$  between control and stretch-exposure groups among samples based on Student's t-test (significance defined as  $P < 0.05$ ).

### *miRNA Target Prediction*

We identified putative mRNA targets of interest for all meaningfully dysregulated miRNAs via the bioinformatics tool TargetScan (<http://www.targetscan.org/>). TargetScan utilizes algorithms to search for complementarity between the miRNA seed sequence and potential mRNA targets. The seed sequence typically consists of bases 2-7 on the 5'-end of the miRNA and exhibits perfect complementarity to the corresponding region of the target mRNA (25).

### *Western Blotting for Protein Analysis of Conditioned Media*

Conditioned medium was collected from cells immediately after exposure to 24 hours of 0-12% cyclic stretch or controls samples. Conditioned medium samples were stored at  $-20^{\circ}\text{C}$  and thawed prior to processing. The conditioned medium was concentrated using StrataClean Resin (Aligent, Santa Clara, CA), reduced with 2-mercaptoethanol in laemmli sample buffer and boiled for 5 minutes at  $90^{\circ}\text{C}$  prior to electrophoresis. 20  $\mu\text{l}$  of each sample were loaded into wells of 10% Mini-Protean TGX Precast Gels (Bio-Rad) and gels were run for 30 minutes at 50V,

followed by 1 hour at 100V. Migrated proteins were transferred to activated PVDF membranes overnight at 30V. Membranes were then blocked in a solution of 5% milk in Tris Buffered Saline (20mM Tris, 0.5M NaCl) with 1% Tween-20 for 2 hours before being cut and incubated overnight with primary antibodies for TGF $\beta$ 2, collagen I, collagen IV, collagen VI and fibronectin (Table 1). Membranes were washed and stained with appropriate secondary antibodies conjugated to horseradish peroxidase for 1 hour prior to being imaged via chemiluminescence reaction using SuperSignal West Femto substrate solution (ThermoFisher). Images were captured using a Fluorchem 8900 imager (Alpha Innotech, San Leandro, CA). Images were analyzed for optical density using ImageJ. Optical densities for each band were normalized to control values and represented with bar graphs. Note: Conditioned media samples from 4 cell strains were examined. One cell strain from this group is not represented in miRNA analysis due to lack of adequate total RNA.

<b>1° Antibody</b>	<b>Host Animal</b>	<b>Catalog #</b>	<b>Source</b>	<b>Dilution</b>
TGF $\beta$ 2	Mouse	Ab36495	Abcam	1:1000
Fibronectin	Rabbit	Ab2913	Abcam	1:1000
Collagen I	Rabbit	Ab34710	Abcam	1:1000
Collagen IV	Rabbit	Ab4500369	Abcam	1:1000
Collagen VI	Rabbit	Ab6588	Abcam	1:1000

**Table 1. Primary Antibody Information**

## **Results**

### *miRNA Expression Profiles*

SYBR Green-based real-time miRNA PCR arrays were used to examine the expression of both profibrotic and anti-fibrotic miRNAs from three normal ONHA cell cultures exposed to 0-12% cyclic stretch for 24 hours. The differential miRNA expression profiles for each of the 3 ONHA groups examined are displayed in Figure 3. There were no statistically significant differences in the expression fold changes of any miRNAs among the stretch-exposed and control groups. The up and downregulation of some miRNAs examined may still be biologically meaningful and the data demonstrated consistent patterns of dysregulation in ONHA exposed to cyclic stretch. In all the miRNA profiles, miR-661 and miR-146b-5p were consistently upregulated; miR-21-5p, miR-29c-3p and miR-26b-5p were consistently downregulated. The average fold change for the expression of these miRNAs among the three ONHA groups is noted in Figure 3, Table E.

### *miRNA Target Predictions*

For the miRNAs that demonstrated consistent patterns of dysregulation, TargetScan was utilized to identify putative mRNA targets. Predicted targets for each miRNA of interest that are directly related to the regulation or composition of the extracellular matrix are listed in Table 2.

### *Conditioned Medium Western Blots*

Conditioned medium was collected from cell cultures used in stretch experiments. Secreted proteins were assessed using western blotting for TGF $\beta$ 2 and multiple ECM proteins – fibronectin, collagen I, collagen IV, and collagen VI. TGF $\beta$ 2, a regulator of ECM protein expression was detected at 50 kDa, 25 kDa and 12.5 kDa representing the latent complex (TGF $\beta$ 2 bound to latency associated peptide), dimer and monomer, respectively. TGF $\beta$ 2 protein levels were induced in three of the four groups examined when exposed to cyclic stretch compared to controls. Fibronectin appears to be slightly elevated in three of the four ONHA groups examined. There are apparent differences in the band densities for some collagen proteins, but these differences are not reproducible across ONHA groups (Figure 4). Semiquantitative representations of individual band densities for each ONHA group are depicted in Figure 5.

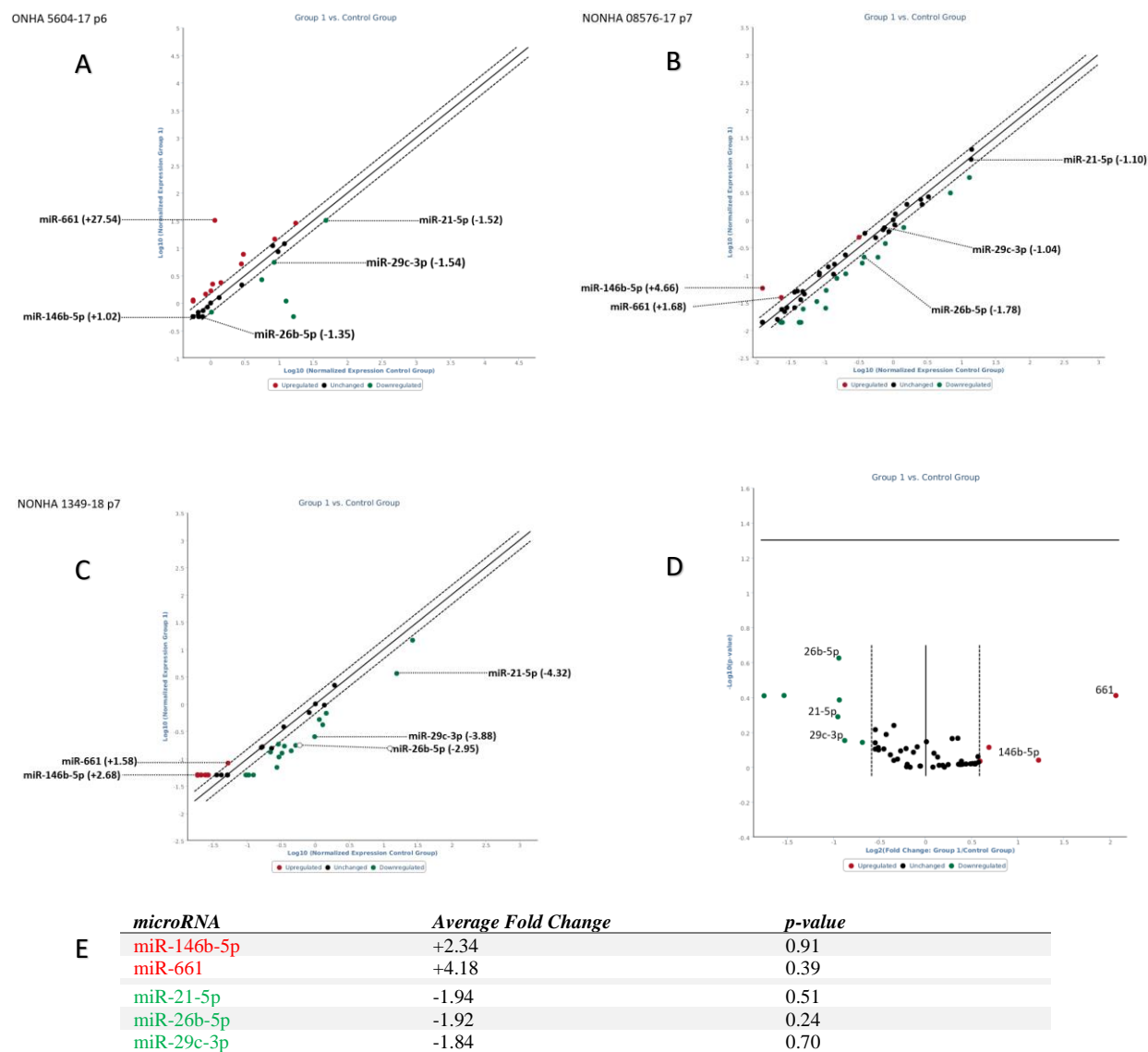


**Figure 3. Differential mature miRNA expression patterns detected in three independent primary human ONHA cell cultures exposed to 0-12% cyclic stretch for 24 hours.**

**A,B,C:** Scatter plots generated by the Qiagen GeneGlobe Analysis software for mature miRNA profiling. Graphs represent normalized expression data for ONHA exposed to 0-12% cyclic stretch plotted against controls. Dashed parallel lines demarcate a 1.5-fold threshold with red data points indicating upregulated miRNAs and green data points indicating downregulated miRNAs. Data normalized using expression of the SNORD96A housekeeping gene. **D:** Volcano plot depicting composite miRNA expression patterns of all ONHA groups (n=3). Solid horizontal line indicates threshold for statistical significance ( $p=0.05$ ), with points above the line being statistically significant. **E:** Composite fold change and  $p$ -values for all miRNAs that were consistently up or down-regulated across ONHA groups (n=3).  $p$ -values based on Student's t-test.

	<b>miRNA</b>	<b>Predicted mRNA Targets</b>
Upregulated	miR-146b-5p	Matrix Metalloproteinase 16, SMAD4
	miR-661	Gremlin 1, Matrix Metalloproteinase 2, TGFβ1, TGFβR associated protein 1, TGFβ-activated kinase, Elastin, Fibronectin type III Domain, Collagen (I, II, IV, V, VI, VII, IX, XII, XVII, XX, XXIII, XXVI α-subunits)
Downregulated	miR-21-5p	Fibroblast Growth Factor (7, 18, 23) TGFβ-induced, TGFβ2R, Matrilin 2, TIMP Metalloproteinase Inhibitor 3, SMAD7, Jagged 1, Collagen IV α1
	miR-26b-5p	Lysyl oxidase-like 2, SMAD1, Jagged 1, Latent TGFβ Binding Protein 1, TGFβ Activated Kinase 1, BMP2 Inducible Kinase, Lysyl Hydroxylase 2, Hyaluronan Synthase 2, ADAM Metalloproteinase Domain 17 & 19, Matrix Metalloproteinase 16, Collagen (I, V, IX, X, XI, XIX, XXII α-subunits)
	miR-29c-3p	Lysyl Oxidase-like 2 & 4, SMAD Nuclear Interacting Protein 1, TGFβ-induced Factor, BMP1, Hyaluronan and Proteoglycan Link Protein 1 & 3, Hyaluronan Synthase 3, Elastin, Fibrillin 1, Collagen (I, II, III, IV, V, VI, VII, IX, XI, XII, XV, XVI, XIX, XXII, XXV, XXVII α-subunits), Matrix Metalloproteinase 24, ADAM Metalloproteinase 1, Fibroblast Growth Factor Receptor Substrate 2, Fibrosin

**Table 2. Dysregulated miRNAs and Predicted Targets.**

List of predicted mRNA targets for the five miRNAs of interest identified in this study. mRNAs listed encode proteins that make up the ECM or are involved in its regulation and remodeling.

Red – miRNAs upregulated; green – miRNAs downregulated.

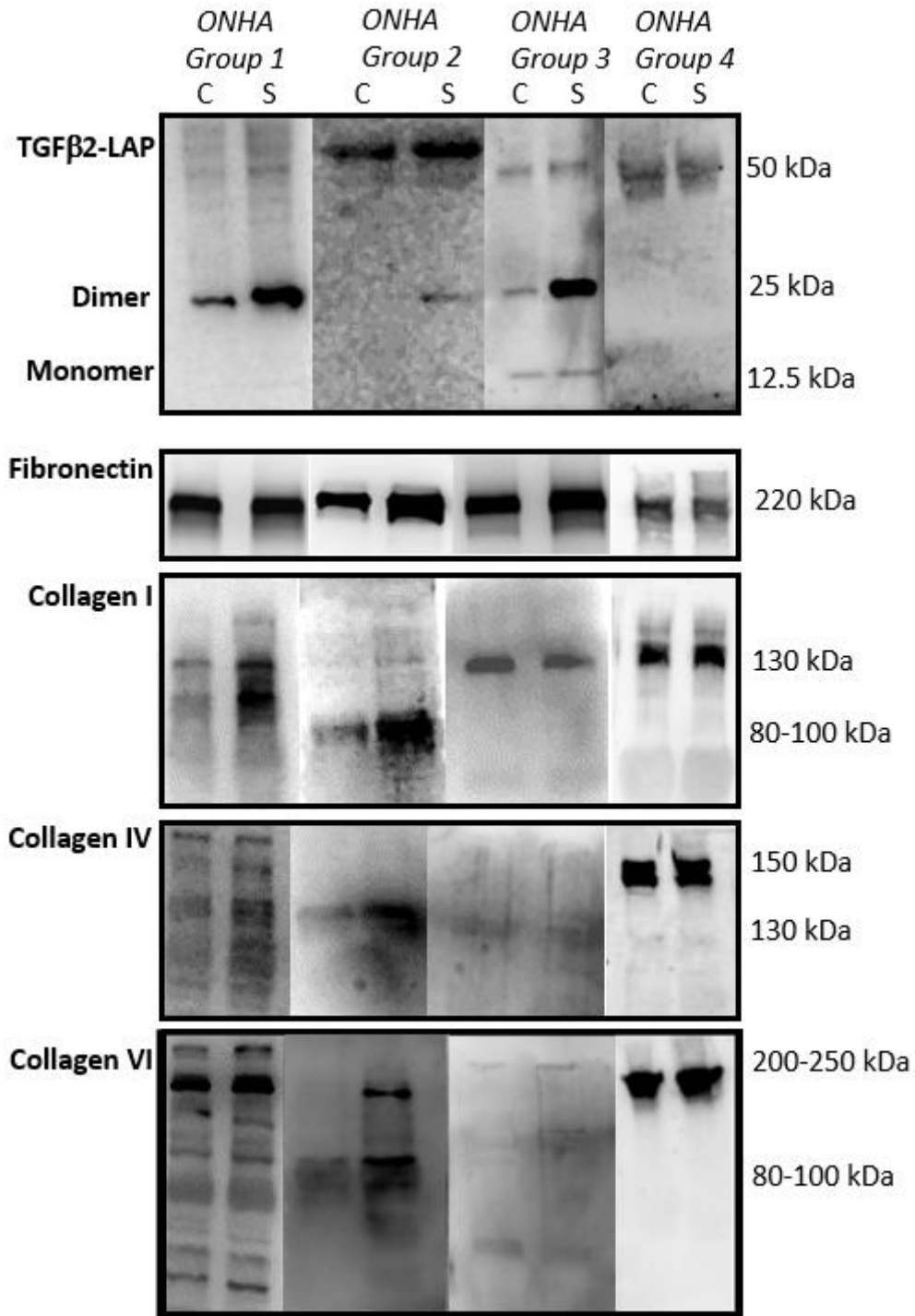


**Figure 4. Western Blot Results**

Western blot analysis of secreted proteins in ONHA. Culture conditioned medium was analyzed for TGFβ2, fibronectin, collagens I, IV, and VI. C annotates samples from control groups exposed without stretch, S annotates samples from groups exposed with 0-12% cyclic stretch for 24 hours (n=4).

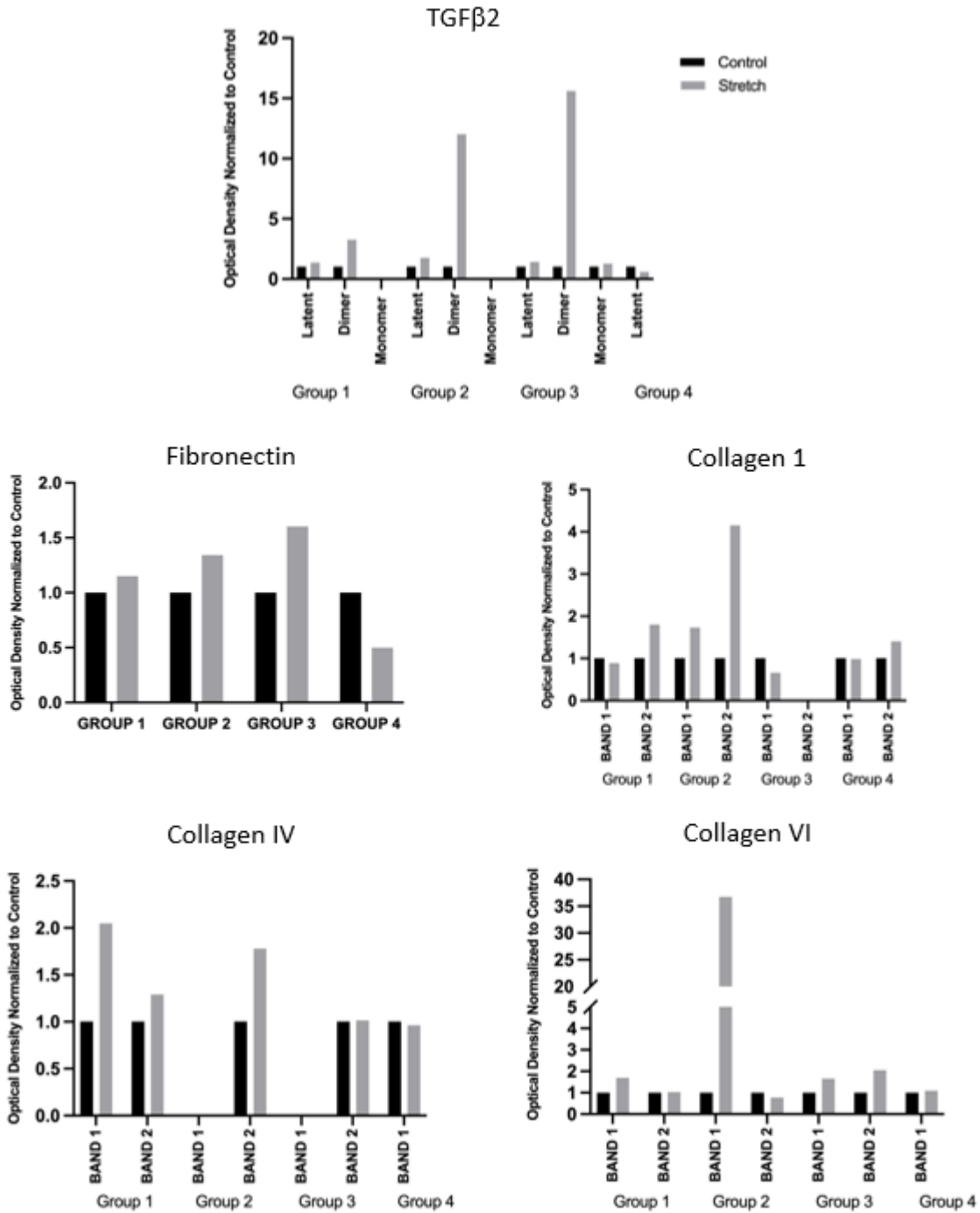


**Figure 5. Western Blot Optical Density Quantitation**

Semi-quantitative optical density readings for corresponding western blots displayed in Figure 4. Density results for observed bands of interest (with kDa values highlighted in Figure 4) were normalized to the value of control bands. Results are displayed for each ONHA group independently. Black = control band value; Grey = 0-12% stretch band value.

## **Discussion**

We have found that miRNAs are differentially expressed after exposure to cyclic stretch in human ONHA. Although we did not find any statistically significant changes in the miRNA expression profiles of ONHA exposed to cyclic stretch, five miRNAs demonstrated consistent patterns of dysregulation and may have biologically meaningful roles in ONH ECM dysregulation. In addition, using TargetScan, we identified putative mRNA targets for these five miRNAs of interest, which included profibrotic factors. Finally, we have demonstrated that ONHA secrete increased levels of TGF $\beta$ 2 after exposure to cyclic stretch when compared to controls.

miRNAs and their target mRNAs are involved in regulating the synthesis and turnover of ECM proteins. We observed certain miRNAs seem to be consistently up or downregulated when ONHA are exposed to cyclic stretch. Using target prediction tools, these miRNAs are predicted to target the mRNAs encoding for multiple ECM proteins involved in ECM regulatory pathways such as the TGF $\beta$ /SMAD pathways. Targets also included matrix metalloproteases, which are involved in the biochemical processes that regulate ECM turnover and remodeling. These putative targets indicate that the miRNA expression changes observed are likely to be biologically relevant to the pathological fibrosis observed at the LC during glaucoma progression. Fibrosis is a physiologic process involved in tissue repair. If uncontrolled, fibrosis can become pathologic and is characterized by a marked increase in the deposition of ECM proteins (26). The ECM of the trabecular meshwork (TM), cornea, sclera and LC of the eye are all composed of a similar profile of proteins, especially collagens. During glaucoma progression, the TM and LC are particularly prone to profibrotic changes that increase tissue stiffness (27).

ECM crosslinking proteins are a driver of increased stiffness in the LC and TM, especially the lysyl oxidase and lysyl oxidase-like family of proteins responsible for crosslinking the abundant fibrillar collagen chains present in the ECM of these tissues (27). Lysyl oxidase-like 2 was the predicted target of both miR-29c-3p and miR-26b-5p, two of the three downregulated miRNAs examined. If these miRNAs substantially reduce the expression of lysyl oxidase-like proteins under normal conditions, their downregulation in ONHA facing biomechanical insults may contribute to an increase in collagen crosslinking and, in turn, increased tissue stiffness at the LC.

Another important promoter of fibrosis is elevated levels of TGF $\beta$  (28). In its canonical pathway, mature TGF $\beta$  interacts with TGF $\beta$  receptors (TGF $\beta$ R) which phosphorylate receptor-regulated SMAD proteins (R-SMADs). R-SMADS form a trimeric complex with SMAD4 and act as transcriptional activators for many genes involved in the maintenance of the ECM (29). All of the miRNAs of interest examined in this study have predicted targets in the TGF $\beta$ 2/SMAD pathway, suggesting that their dysregulation has the potential to modulate the expression of ECM genes in ONHA. miRNAs with targets in the TGF $\beta$  pathway have the potential to be exploited to lessen the severity of the profibrotic molecular changes observed under glaucomatous conditions. In glaucomatous human ONH tissue, TGF $\beta$ 2 is the predominant TGF $\beta$  isoform and is overexpressed by ~100-fold in comparison to healthy tissue (30) and TGF $\beta$ 2 demonstrably increases the expression of ECM constituents in cells of the LC (31). In previous work from our lab, it was demonstrated that LC cells treated with TGF $\beta$ 2 produced more collagen types I and IV, but transfection of a miR-29c mimic attenuated this TGF $\beta$ 2-induced collagen expression (unpublished).

We expected that miRNAs upregulated in ONHA exposed to cyclic stretch would be profibrotic and miRNAs observed to be downregulated would be anti-fibrotic. In our study, downregulated miRNAs (miR-21-5p, miR-26b-5p, miR-29c-3p) examined had predicted fibrotic mRNA targets suggestive of strongly anti-fibrotic activity. However, the two upregulated miRNAs (miR-146b-5p and miR-661) examined also appear to have many targets that should confer anti-fibrotic activity. For example, miR-661 is predicted to target gremlin-1. Gremlin-1 is an antagonist of bone morphogenetic protein (BMP), which is in-turn an antagonist of TGF $\beta$  signaling pathway. Should miR-661 meaningfully downregulate gremlin, it would promote the BMP induced inhibition of TGF $\beta$  - this would be an anti-fibrotic effect. Importantly, elevated expression of gremlin has been experimentally demonstrated to promote ECM deposition by TM cells (32). In contrast, miR-146b-5p is upregulated in response to pro-inflammatory cytokines in ocular tissues (33) and is a hypoxia-induced promoter of fibrosis in myocardial tissues (34). This highlights a need to validate our target predictions and experimentally characterize the biological effects of individual miRNAs to properly assess our initial hypothesis.

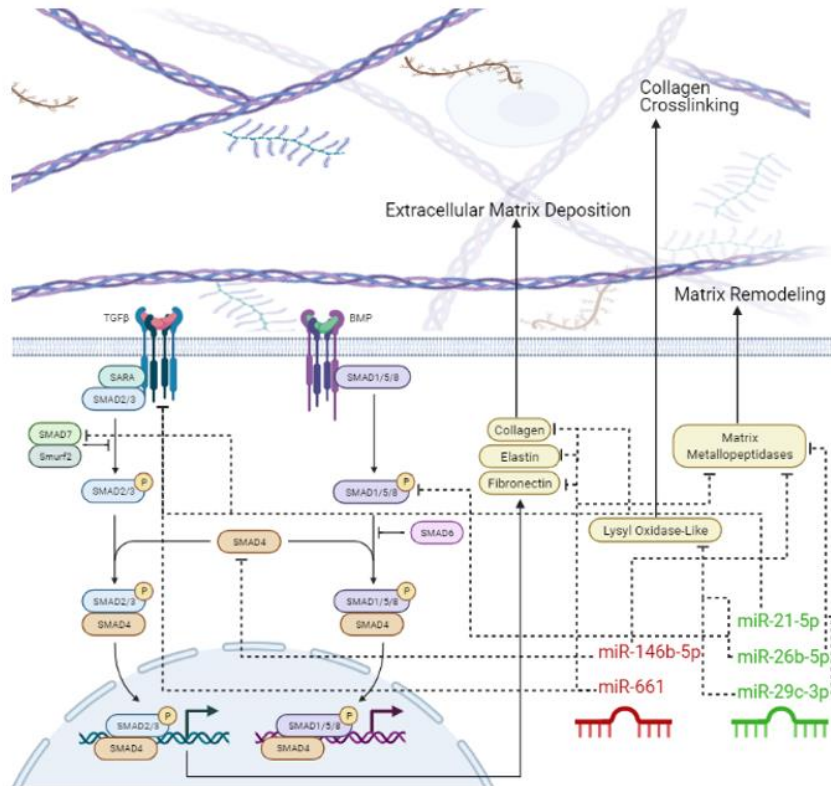


**Figure 6. Predicted miRNA Interactions**

Predicted interactions between miRNAs of interest and targets in canonical fibrotic pathways. Created with BioRender.com

In examining the many potential mRNA targets for each miRNA of interest, it is reasonable to question the value of miRNAs as models for novel therapeutics. miRNAs may have unclear mechanisms of actions and many off-target or undesirable effects. But, the ability of individual miRNAs to modulate the activity of a variety of targets may also be an advantage in attenuating the pathological phenotypes of diseases with complex etiologies (35). For example, miR-26b-5p has been demonstrated to inhibit fibrosis in the lens of the eye through inhibition of SMAD4 and through inhibition of Jagged-1 (36,37). Also, miR-26b may prevent microglial activation and neurotoxicity in neural tissues under ischemic conditions through inhibition of interleukin 6 (38), and may help prevent ischemic damage in tissues by promoting angiogenesis through the inhibition of PTEN in endothelial cells (39). These issues of fibrosis, glia-mediated neurotoxicity

and ischemia are all relevant to the glaucomatous pathology observed in the ONH and demonstrate how miRNAs have the potential to be therapeutic through multiple mechanisms of action.

We believe our data support our hypothesis that biomechanical forces at the LC drive miRNA dysregulation in ONHA, contributing to pathological ECM remodeling and overexpression of profibrotic factors. Although we have not yet been able to detect statistically significant dysregulation in our miRNA profiles, it is clear that these data have the potential to be biologically meaningful. Further research characterizing the effects of the miRNAs discussed in this report on ONHA and other ONH cell populations is warranted.

## **Limitations**

A major limitation of this study was the sample size (n=3). Time constraints prevented the analysis of additional human primary ONHA cell strains as primary ONHA often grow slowly, exhaust quickly after repeated passaging, and a large number of cells are required to obtain high-quality total RNA samples. Given the degree of variability seen in our miRNA expression fold-change data, a sample size of 3 likely did not confer enough power to detect any significant expression changes. Additionally, the need to use a large number of cells for RNA extraction prevented us from extracting any other cell lysates for other analyses.

Another limitation in our study is the use of only one parameter for stretch. Some studies suggest that physiologic levels of strain may reach up to 1% in ocular tissues associated with the optic nerve, with pathophysiological responses occurring once strain exceeds 3.5% (40). In our study, the use of 0-12% cyclic stretch should be sufficient to produce a biologically meaningful response. This is supported by our western blot data, which showed cyclic stretch stimulated the secretion of TGF $\beta$ 2 in ONHA. These results are consistent with the data from other studies that have shown 15% transient stretch reliably increases TGF $\beta$ 2 mRNA and protein levels in cells of the LC (31). However, we cannot determine how responses might differ if ONHA were exposed to lower or higher levels of strain – as might occur during the earlier or later stages of glaucoma progression, respectively. This could be an area for investigation in future studies. Furthermore, stretch cannot fully mimic the complex biomechanical distortions that occur in the LC during glaucoma (40).

Limitations also exist in our ability to predict the targets and effects of the miRNAs under examination. miRNAs exhibit a diverse array of regulatory functions (18). The methods of this

study limit us to only predict targets of miRNAs' canonical post-transcriptional activities, but this may not represent the totality of their function. miRNAs can imperfectly base pair with and “target” multiple unique mRNA molecules (18). This can make an accurate prediction of mRNA targets difficult. TargetScan's algorithm, which bases its predictions mainly on the seed region of miRNAs (which base pairs perfectly with the corresponding region of their mRNA targets), is a relatively robust bioinformatics tool. However, it still produces a false positive rate of around 22% and cannot predict every valid mRNA target for a given miRNA (41). Therefore, the experimental validation of miRNAs with miRNA mimics and inhibitors are important for a complete interpretation of data produced by miRNA profiling. Neither the experimental validation of miRNA targets nor the characterization of miRNA effects through the use of miRNA mimics and inhibitors were utilized in this study due to this one-year program's time constraints.

## **References**

1. Quigley H. A. (1993). Open-angle glaucoma. *The New England journal of medicine*, 328(15), 1097–1106. <https://doi.org/10.1056/NEJM199304153281507>
2. Quigley H. A. (2011). Glaucoma. *Lancet (London, England)*, 377(9774), 1367–1377. [https://doi.org/10.1016/S0140-6736\(10\)61423-7](https://doi.org/10.1016/S0140-6736(10)61423-7)
3. Sommer, A., Tielsch, J. M., Katz, J., Quigley, H. A., Gottsch, J. D., Javitt, J., & Singh, K. (1991). Relationship between intraocular pressure and primary open angle glaucoma among white and black Americans. The Baltimore Eye Survey. *Archives of ophthalmology (Chicago, Ill. : 1960)*, 109(8), 1090–1095. <https://doi.org/10.1001/archoph.1991.01080080050026>
4. Weinreb, R. N., Aung, T., & Medeiros, F. A. (2014). The pathophysiology and treatment of glaucoma: a review. *JAMA*, 311(18), 1901–1911. <https://doi.org/10.1001/jama.2014.3192>
5. Quigley, H. A., Addicks, E. M., Green, W. R., & Maumenee, A. E. (1981). Optic nerve damage in human glaucoma. II. The site of injury and susceptibility to damage. *Archives of ophthalmology (Chicago, Ill. : 1960)*, 99(4), 635–649.
6. Tan, N. Y., Koh, V., Girard, M. J., & Cheng, C. Y. (2018). Imaging of the lamina cribrosa and its role in glaucoma: a review. *Clinical & experimental ophthalmology*, 46(2), 177–188. <https://doi.org/10.1111/ceo.13126>
7. Lopez, N. N., Clark, A. F., & Tovar-Vidales, T. (2020). Isolation and characterization of human optic nerve head astrocytes and lamina cribrosa cells. *Experimental eye research*, 197, 108103. <https://doi.org/10.1016/j.exer.2020.108103>
8. Cordeiro, M. F., Chang, L., Lim, K. S., Daniels, J. T., Pleass, R. D., Siriwardena, D., & Khaw, P. T. (2000). Modulating conjunctival wound healing. *Eye (London, England)*, 14 ( Pt 3B), 536–547. <https://doi.org/10.1038/eye.2000.141>
9. Fuchshofer, R., & Tamm, E. R. (2012). The role of TGF- $\beta$  in the pathogenesis of primary open-angle glaucoma. *Cell and tissue research*, 347(1), 279–290. <https://doi.org/10.1007/s00441-011-1274-7>
10. Kirwan, R. P., Leonard, M. O., Murphy, M., Clark, A. F., & O'Brien, C. J. (2005). Transforming growth factor-beta-regulated gene transcription and protein expression in human GFAP-negative lamina cribrosa cells. *Glia*, 52(4), 309–324. <https://doi.org/10.1002/glia.20247>
11. Hernandez, M. R., Miao, H., & Lukas, T. (2008). Astrocytes in glaucomatous optic neuropathy. *Progress in brain research*, 173, 353–373. [https://doi.org/10.1016/S0079-6123\(08\)01125-4](https://doi.org/10.1016/S0079-6123(08)01125-4)

12. Liu, B., Chen, H., Johns, T. G., & Neufeld, A. H. (2006). Epidermal growth factor receptor activation: an upstream signal for transition of quiescent astrocytes into reactive astrocytes after neural injury. *The Journal of neuroscience : the official journal of the Society for Neuroscience*, 26(28), 7532–7540.  
<https://doi.org/10.1523/JNEUROSCI.1004-06.2006>
13. Hopkins, A. A., Murphy, R., Irnaten, M., Wallace, D. M., Quill, B., & O'Brien, C. (2020). The role of lamina cribrosa tissue stiffness and fibrosis as fundamental biomechanical drivers of pathological glaucoma cupping. *American journal of physiology. Cell physiology*, 319(4), C611–C623.  
<https://doi.org/10.1152/ajpcell.00054.2020>
14. Yang, J. L., Neufeld, A. H., Zorn, M. B., & Hernandez, M. R. (1993). Collagen type I mRNA levels in cultured human lamina cribrosa cells: effects of elevated hydrostatic pressure. *Experimental eye research*, 56(5), 567–574.  
<https://doi.org/10.1006/exer.1993.1070>
15. Quill, B., Docherty, N. G., Clark, A. F., & O'Brien, C. J. (2011). The effect of graded cyclic stretching on extracellular matrix-related gene expression profiles in cultured primary human lamina cribrosa cells. *Investigative ophthalmology & visual science*, 52(3), 1908–1915. <https://doi.org/10.1167/iovs.10-5467>
16. Hernandez, M. R., Pena, J. D., Selvidge, J. A., Salvador-Silva, M., & Yang, P. (2000). Hydrostatic pressure stimulates synthesis of elastin in cultured optic nerve head astrocytes. *Glia*, 32(2), 122–136. [https://doi.org/10.1002/1098-1136\(200011\)32:2<122::aid-glia20>3.0.co;2-j](https://doi.org/10.1002/1098-1136(200011)32:2<122::aid-glia20>3.0.co;2-j)
17. Rogers, R. S., Dharsee, M., Ackloo, S., Sivak, J. M., & Flanagan, J. G. (2012). Proteomics analyses of human optic nerve head astrocytes following biomechanical strain. *Molecular & cellular proteomics : MCP*, 11(2), M111.012302.  
<https://doi.org/10.1074/mcp.M111.012302>
18. Catalanotto, C., Cogoni, C., & Zardo, G. (2016). MicroRNA in Control of Gene Expression: An Overview of Nuclear Functions. *International journal of molecular sciences*, 17(10), 1712. <https://doi.org/10.3390/ijms17101712>
19. Chendrimada, T. P., Gregory, R. I., Kumaraswamy, E., Norman, J., Cooch, N., Nishikura, K., & Shiekhattar, R. (2005). TRBP recruits the Dicer complex to Ago2 for microRNA processing and gene silencing. *Nature*, 436(7051), 740–744.  
<https://doi.org/10.1038/nature03868>
20. MacRae, I. J., Ma, E., Zhou, M., Robinson, C. V., & Doudna, J. A. (2008). In vitro reconstitution of the human RISC-loading complex. *Proceedings of the National Academy of Sciences of the United States of America*, 105(2), 512–517.  
<https://doi.org/10.1073/pnas.0710869105>

21. O'Reilly S. (2016). MicroRNAs in fibrosis: opportunities and challenges. *Arthritis research & therapy*, 18, 11. <https://doi.org/10.1186/s13075-016-0929-x>
22. Sharma, S., & Lu, H. C. (2018). microRNAs in Neurodegeneration: Current Findings and Potential Impacts. *Journal of Alzheimer's disease & Parkinsonism*, 8(1), 420. <https://doi.org/10.4172/2161-0460.1000420>
23. Hébert, S. S., Horré, K., Nicolai, L., Papadopoulou, A. S., Mandemakers, W., Silahatoglu, A. N., Kauppinen, S., Delacourte, A., & De Strooper, B. (2008). Loss of microRNA cluster miR-29a/b-1 in sporadic Alzheimer's disease correlates with increased BACE1/beta-secretase expression. *Proceedings of the National Academy of Sciences of the United States of America*, 105(17), 6415–6420. <https://doi.org/10.1073/pnas.0710263105>
24. Luna, C., Li, G., Qiu, J., Epstein, D. L., & Gonzalez, P. (2011). Cross-talk between miR-29 and transforming growth factor-betas in trabecular meshwork cells. *Investigative ophthalmology & visual science*, 52(6), 3567–3572. <https://doi.org/10.1167/iovs.10-6448>
25. Lewis, B. P., Burge, C. B., & Bartel, D. P. (2005). Conserved seed pairing, often flanked by adenosines, indicates that thousands of human genes are microRNA targets. *Cell*, 120(1), 15–20. <https://doi.org/10.1016/j.cell.2004.12.035>
26. Wynn T. A. (2008). Cellular and molecular mechanisms of fibrosis. *The Journal of pathology*, 214(2), 199–210. <https://doi.org/10.1002/path.2277>
27. Rahman N., O'Neil E., Irnaten M., Wallace D., O'brien C. (2020). Corneal stiffness and collagen cross-linking proteins in glaucoma: Potential for novel therapeutic strategy. *Journal of Ocular Pharmacology and Therapeutics*, 36(8). <https://doi.org/10.1089/jop.2019.0118>
28. Wordinger, R. J., Fleenor, D. L., Hellberg, P. E., Pang, I. H., Tovar, T. O., Zode, G. S., Fuller, J. A., & Clark, A. F. (2007). Effects of TGF-beta2, BMP-4, and gremlin in the trabecular meshwork: implications for glaucoma. *Investigative ophthalmology & visual science*, 48(3), 1191–1200.
29. Shi, Y., & Massagué, J. (2003). Mechanisms of TGF-beta signaling from cell membrane to the nucleus. *Cell*, 113(6), 685–700. [https://doi.org/10.1016/s0092-8674\(03\)00432-x](https://doi.org/10.1016/s0092-8674(03)00432-x)
30. Pena, J. D., Taylor, A. W., Ricard, C. S., Vidal, I., & Hernandez, M. R. (1999). Transforming growth factor beta isoforms in human optic nerve heads. *The British journal of ophthalmology*, 83(2), 209–218. <https://doi.org/10.1136/bjo.83.2.209>
31. Kirwan, R. P., Fenerty, C. H., Crean, J., Wordinger, R. J., Clark, A. F., & O'Brien, C. J. (2005). Influence of cyclical mechanical strain on extracellular matrix gene expression in human lamina cribrosa cells in vitro. *Molecular vision*, 11, 798–810.

32. Wordinger, R. J., Fleenor, D. L., Hellberg, P. E., Pang, I. H., Tovar, T. O., Zode, G. S., Fuller, J. A., & Clark, A. F. (2007). Effects of TGF-beta2, BMP-4, and gremlin in the trabecular meshwork: implications for glaucoma. *Investigative ophthalmology & visual science*, 48(3), 1191–1200. <https://doi.org/10.1167/iovs.06-0296>
33. Kutty, R. K., Nagineni, C. N., Samuel, W., Vijayasarathy, C., Jaworski, C., Duncan, T., Cameron, J. E., Flemington, E. K., Hooks, J. J., & Redmond, T. M. (2013). Differential regulation of microRNA-146a and microRNA-146b-5p in human retinal pigment epithelial cells by interleukin-1 $\beta$ , tumor necrosis factor- $\alpha$ , and interferon- $\gamma$ . *Molecular vision*, 19, 737–750.
34. Liao, Y., Li, H., Cao, H., Dong, Y., Gao, L., Liu, Z., Ge, J., & Zhu, H. (2021). Therapeutic silencing miR-146b-5p improves cardiac remodeling in a porcine model of myocardial infarction by modulating the wound reparative phenotype. *Protein & cell*, 12(3), 194–212. <https://doi.org/10.1007/s13238-020-00750-6>
35. Hanna, J., Hossain, G. S., & Kocerha, J. (2019). The Potential for microRNA Therapeutics and Clinical Research. *Frontiers in genetics*, 10, 478. <https://doi.org/10.3389/fgene.2019.00478>
36. Dong, N., Xu, B., Benya, S. R., & Tang, X. (2014). MiRNA-26b inhibits the proliferation, migration, and epithelial-mesenchymal transition of lens epithelial cells. *Molecular and cellular biochemistry*, 396(1-2), 229–238. <https://doi.org/10.1007/s11010-014-2158-4>
37. Chen, X., Xiao, W., Chen, W. *et al.* (2017). MicroRNA-26a and -26b inhibit lens fibrosis and cataract by negatively regulating Jagged-1/Notch signaling pathway. *Cell Death Differ* 24, 1431–1442. <https://doi.org/10.1038/cdd.2016.152>
38. Kang, Y. C., Zhang, L., Su, Y., Li, Y., Ren, W. L., & Wei, W. S. (2018). MicroRNA-26b Regulates the Microglial Inflammatory Response in Hypoxia/Ischemia and Affects the Development of Vascular Cognitive Impairment. *Frontiers in cellular neuroscience*, 12, 154. <https://doi.org/10.3389/fncel.2018.00154>
39. Martello, A., Mellis, D., Meloni, M., Howarth, A., Ebner, D., Caporali, A., & Al Haj Zen, A. (2018). Phenotypic miRNA Screen Identifies miR-26b to Promote the Growth and Survival of Endothelial Cells. *Molecular therapy. Nucleic acids*, 13, 29–43. <https://doi.org/10.1016/j.omtn.2018.08.006>
40. Sigal, I. A., Flanagan, J. G., Tertinegg, I., & Ethier, C. R. (2004). Finite element modeling of optic nerve head biomechanics. *Investigative ophthalmology & visual science*, 45(12), 4378–4387. <https://doi.org/10.1167/iovs.04-0133>

41. Min, H., & Yoon, S. (2010). Got target? Computational methods for microRNA target prediction and their extension. *Experimental & molecular medicine*, 42(4), 233–244.  
<https://doi.org/10.3858/emm.2010.42.4.032>